Draft version January 28, 2012
Preprint typeset using LaTeX style emulateapj v. 08/22/09

GALAXY EVOLUTION IN THE DEEP LENS SURVEY: II. THE BUTCHER-OEMLER EFFECT IN 302 CLUSTERS

R. Voss[1,2], C. Esmerian, V. Margoniner[1], D. Wittman[2]

Draft version January 28, 2012

ABSTRACT

In this paper we investigate the Butcher-Oemler effect in a sample of 302 newly-detected galaxy clusters in the Deep Lens Survey, in an attempt to gain a deeper understanding of the fundamental mechanisms involved in galaxy and cluster evolution. We use $BVRz'$ CCD photometry to confirm the presence of the Butcher-Oemler effect in clusters out to redshift $z = 0.80$, with blue population increasing linearly with redshift. Throughout this study, we compare clusters of similar redshift, richness, and concentration, and examine how these properties contribute to their observed color evolution. Although we find redshift to be the primary factor in determining a cluster's blue fraction, concentration and passive evolution are found to be secondary parameters. We conclude that the Butcher-Oemler effect is likely a consequence of frequent galaxy-galaxy interactions and merging taking place within the densest cluster environments.

Subject headings: galaxies: evolution - galaxies: clusters - galaxies: photometry

1. INTRODUCTION

Galaxy clusters are the largest gravitationally bound structures in the known universe. Comprising of hundreds to thousands of galaxies, these structures have proven to be valuable in our understanding of the fundamental processes that govern galaxy formation and evolution. An important clue as to how galaxies evolve is the discovery that galaxy clusters at high redshifts have a greater population of blue galaxies compared to clusters nearby; a trend known as the Butcher-Oemler effect (Butcher and Oemler 1984).

The Butcher-Oemler effect was first observed in Butcher and Oemler (1978) and later confirmed in Butcher and Oemler (1984) when detailed photometry of 33 galaxy clusters revealed that the relative fraction of blue galaxies (f_B) of these clusters remained constant at $f_B = 0.03\pm0.01$ for $z < 0.1$, and increased with redshift to $f_B = 0.25$ at $z \approx 0.5$. These observations have since been confirmed in a number of studies (Lavery and Henry 1988; Rakos et al. 1996; Ellingson et al. 2001; Margoniner et al. 2001; Tran et al. 2005). This was some of the first evidence suggesting evolutionary processes are at place in the cores of galaxy clusters, and that unseen mechanisms are restricting the rate of star formation in cluster galaxies; resulting in a decline in the blue population over time.

Later studies have shown the f_B of a cluster to correlate with cluster properties such as luminosity (Ellingson et al. 2001), richness (Margoniner et al. 2001), and concentration (Butcher and Oemler 1984), hinting that local environment may be a key factor in determining the size of a cluster's blue population. Direct observations (Lavery and Henry 1988) have revealed an increase in the number of tails, streamers, and other tidal features present on spiral galaxies in rich clusters, suggesting that interactions between cluster members are frequent. Galaxy-galaxy interactions and merging are known to cause bursts of rapid star formation, resulting in an accelerated rate of evolution (Mo et al. 2010). These starburst galaxies use up their star forming material relatively quickly, eventually resulting in a reddening in color as they are unable to form new stars. Detailed spectroscopic measurements of Butcher-Oemler cluster members (Dressler and Gunn 1983) show prominent emission lines of [O$_{II}$],[O$_{III}$], and Hβ; evidence that intense star formation has occurred in the past. Furthermore, Rakos et al. (1996) found an abundance of starburst galaxies in Butcher-Oemler clusters, advancing the idea that merging and galaxy-galaxy interactions are the driving force behind the Butcher-Oemler effect.

However, recent investigations (Ellingson et al. 2001; Tran et al. 2005) have shown that galaxy infall could be the primary mechanism for the decline in the blue-fraction observed in clusters at lower redshifts. Late-type field galaxies located near a cluster's edge can fall into the cluster's core region, and experience a ram-pressure from the inter-cluster medium (ICM), stripping galaxies of their star-forming material (Dressler and Gunn 1983). It has been theorized that these infalling late-type spiral galaxies morph into early-type lenticular galaxies once star formation has ceased, thus giving a likely explanation as to why lenticular galaxies are abundant in the cores of highly-evolved clusters (**?**).

There has been some speculation that cluster galaxies may be passively evolving at a rate comparable to those in the field, and that the Butcher-Oemler effect could primarily be due to an aging stellar population (Andreon 2006). As galaxies age, the blue star population will deminish, yeilding an abundance of old red stars; leaving the galaxy with a reddened appearance.

In this study we aim to verify the existence of the Butcher-Oemler effect, and investigate the influences of merging, infall, and passive galactic evolution on cluster blue fraction. We analyze the blue galaxy populations in clusters of similar richness, concentration, and redshift as to not introduce a bias from comparing clusters

[1] Department of Physics, California State University at Sacramento, 6000 J Street, Sacramento, CA 95826
[2] Department of Physics, University of California at Davis, 1 Shields Avenue, Davis, CA 95616

with different properties. The layout of this paper is as follows: In §2 we cover the specifications of the Deep Lens Survey, photometric redshifts, creation of our cluster sample, and estimation of the background field. §3 we analyze the Butcher-Oemler effect and how it relates to other cluster properties such as redshift, richness, and concentration. In §4 we discuss the significance of these results, and how they relate to previous works.

2. OBSERVATIONS AND DATA REDUCTION

2.1. *Observations*

The Deep Lens Survey (DLS) is a deep, large-scale imaging survey composed of five 2×2 degree fields. Observing fields were chosen to minimize contamination from bright stars and galactic extinction, and were not selected based on previously known structures (Wittman et al. 2002). The CCD images were obtained using 4-meter telescopes at Kitt Peak National Observatory (KPNO) and Cerro Tololo Inter-American Observatory (CTIO) through Harris BVR and Sloan z' filters. Each CCD has 10,000×10,000 pixels with each pixel corresponding to 0.257 arc-seconds. Twenty exposures were taken with times of 600 seconds in BVz' and 900 seconds in R. Objects were identified and cataloged using SExtractor (Bertin and Arnouts 1996) and magnitudes were obtained with ColorPro (Coe et al. 2006). Roughly 6 million DLS galaxies have been cataloged. Refer to Wittman et al. (2002) for a more in-depth explanation as to the adopted observing methods and specifications of the survey.

Galactic extinction corrections were applied using the $E(B-V)$ map of Schlegel et al. (1998) using 4.325 $E(B-V)$ for the B band, 3.240 $E(B-V)$ for the V band, 2.634 $E(B-V)$ for the R band, and 1.540 $E(B-V)$ for the z' band. All magnitudes are calibrated using the AB system. We used the spectral energy distribution of an elliptical galaxy to derive $k(z)$ corrections, allowing us to compare galaxies at their $B-V$ rest-frame absolute magnitudes. Region masks and exclusion zones were applied around bright stars, saturated objects, and field edges using DS9 (Joye and Mandel 2003).

2.2. *Photometric Redshifts*

Photometric redshifts and galaxy types were estimated using the Bayesian Photometric Redshift Estimation algorithm (BPZ) (Benítez 2000). Only galaxies with BPZ ODDS greater than 0.9 were considered, giving us reliable photometric redshifts without rendering our data sample unusable. We use a simulation of the DLS developed by Margoniner and Wittman (2008) to determine how accurately BPZ detects galaxies of different redshift, type, and color with ODDS > 0.9; resulting in fractions $(\frac{Blue_{Detected}}{Blue_{Simulated}}, \frac{Total_{Detected}}{Total_{Simulated}})$ that we later apply as a correction to the final data (Fig. 1). This correction compensates for fraction galaxies that are cut by the BPZ ODDS at each redshift.

When comparing photometric to previously known spectroscopic redshifts in Field 1, the amount of scatter in the relation is $\Delta z \approx 0.06$ for redshifts $z < 1$ (Margoniner and Wittman 2008). We therefore adopted $\Delta z = 0.06$ as the depth of our redshift range used for determining potential cluster member galaxies.

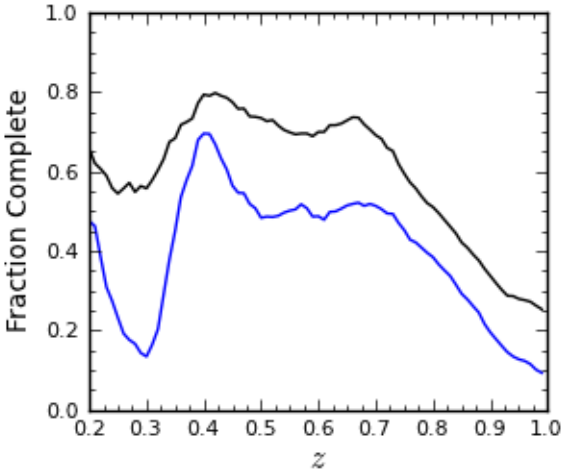

FIG. 1.—: Color completeness of BPZ in a DLS simulation as a function of redshift. The blue line represents the fraction of blue galaxies BPZ detects for ODDS > 0.9, the black line is the fraction of total galaxies BPZ detects for ODDS > 0.9.

2.3. *Cluster Sample*

Galaxy clusters were detected using the Bayesian Cluster Finder (Ascaso et al. 2010), an algorithm that identifies clusters based on three criteria: high density, a defined red-sequence, and luminosity function. By taking advantage of a variety of different detection methods, it has the ability to detect clusters that may not have well-defined red-sequences due to high redshifts, or low richnesses. Furthermore, this algorithm is not subject to the optical selection effects which may have biased the results of previous studies. In all, a total of 845 cluster candidates were detected.

For each candidate, the mean redshift of its cluster members was determined. Cluster richnesses (Λ_{CD}) are defined as the effective number of L^* galaxies in the cluster (Ascaso et al. 2010). This method of richness estimation is dependent on redshift, therefore a correction is applied to account for the fraction of luminosity that is lost due to the apparent depth of the survey. The brightest cluster galaxy (BCG) of each cluster is taken to be the cluster's central coordinates (Dressler 1984).

Similar to richness, we also aim to analyze how cluster blue fraction depends on concentration (C), which we define as the ratio of the effective surface densities within a 0.5 Mpc radius and a 1.5 Mpc radius from a cluster's center.

$$C \equiv \rho(R_{0.5})/\rho(R_{1.5})$$

It is important to note how concentration differs from richness; while richness is a measurement of the total number of cluster members, concentration is a measurement of how dense the central core region is compared to the rest of the cluster. Concentration also gives insight of how the galaxies are distributed within the area of a cluster. A cluster with $C < 1$ means that either, the cluster

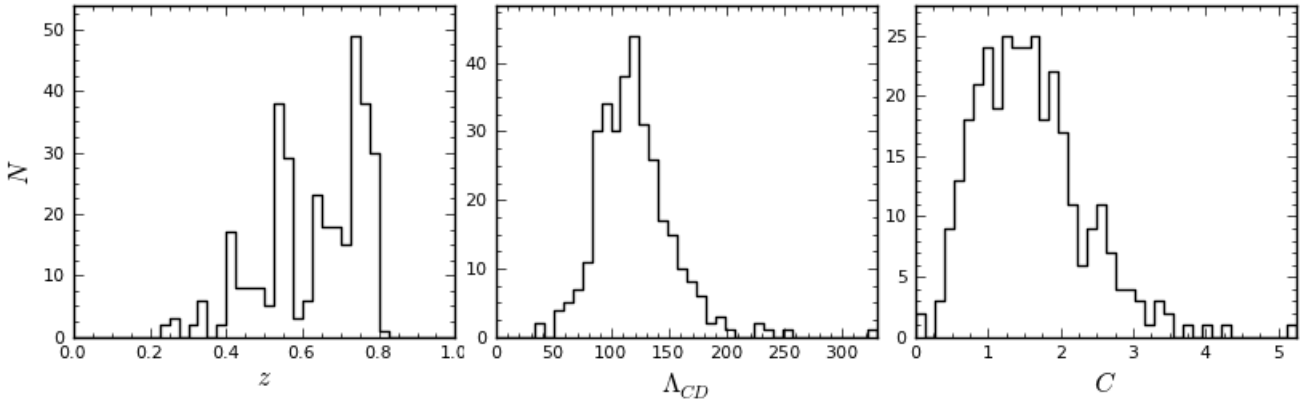

FIG. 2.—: Redshift (z), richness (Λ_{CD}), and concentration (C) distributions of our cluster sample.

has some kind of outer substructure, or a mistaken cluster center. It is evident from Figure **??** that richness and concentration are not correlated for our cluster sample.

In order to obtain an accurate fit to a cluster's red-sequence, only clusters with greater than 5 E/S0 galaxies brighter than a limiting absolute magnitude of $M_v = -20$ were considered (more in §3.1). Clusters having greater than 20% of their area within a masked region, or were too close of proximity to a field's edge regions were discarded. After these cuts were applied to our sample, a total of 302 clusters remained with ranges in redshift from $z = 0.25$ to $z = 0.74$,in richness from $\Lambda_{CD} = 39.12$ to $\Lambda_{CD} = 330.6$, and in concentration from $C = 0.33$ to $C = 5.25$ (Fig. 2).

Cosmological distances were computed using the Cosmology Calculator (Wright 2006) assuming a flat cosmology of $H_0 = 68$ Km s^{-1} Mpc^{-1}, $\Omega_\Lambda = 0.7$, and $\Omega_M = 0.3$.

2.4. *Field Sample*

Not only is it critical to statistically subtract the background and foreground contamination when calculating a cluster's blue fraction, we also want to compare the amount of evolution observed in the cluster to that of the galaxy population in the surrounding field. We run a Monte Carlo simulation for each cluster, generating 25 random field coordinates that are not in close proximity to a known cluster or masked region. Each of the 25 coordinates acts as a center-point for a cluster-sized field sample of the same redshift as the subject cluster. We perform the same procedure for these field samples as the true data. This provides accurate representations of the surrounding field population at the same redshifts as the clusters. To minimize the probabilitiy of accidentally landing on an unidentified cluster or substructure, we only use field samples with less total galaxies than in our clusters and with concentrations $0.80 < C < 1.20$.

3. ANALYSIS OF THE BUTCHER-OEMLER EFFECT

3.1. *Calculating the Blue-Fraction*

When studying the Butcher-Oemler effect, it is essential to compare galaxy clusters over a wide range of redshifts. Due to the depth of the survey, observations of high-redshift clusters are limited to only the most luminous galaxies, which is why a fixed absolute magnitude limit is needed. For the purpose of directly comparing our data and results with previous works (Butcher and Oemler 1984; Margoniner et al. 2001), we adopt the original magnitude limit used by Butcher and Oemler of M_v = -20. This gives us a completion out to $z \approx 0.80$ in the DLS.

In Butcher and Oemler (1984), f_B was originally defined as the fraction of galaxies that reside within a radius encompassing 30% of the total cluster population (R_{30}), and having an absolute magnitude brighter than M_v = -20, and a $B - V$ value 0.2 magnitudes bluer than the best linear fit of the cluster's early-type population (red-sequence). We define f_B in a similar way, however we used a fixed radius of 1.5Mpc ($R_{1.5}$) instead of R_{30}. We examine how the galaxy population changes as a function of radius for the top 10% richest and poorest clusters between $0.525 < z < 0.575$, the most populated redshift in our sample. We find that the radial profiles of the two

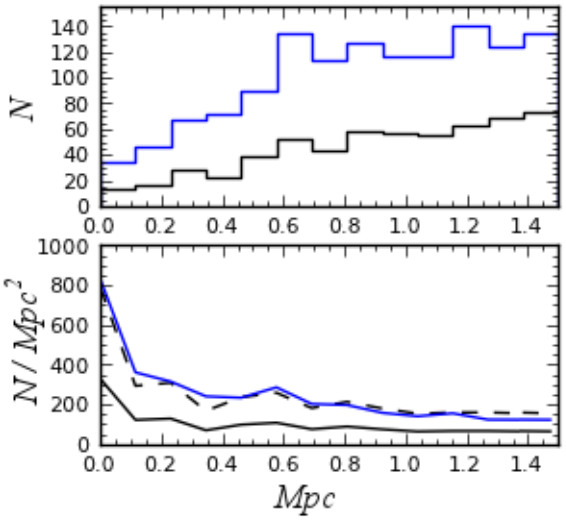

FIG. 3.—: The radial profiles of the richest 10% (blue), and poorest 10% (black) clusters in our sample within a tight redshift range of $0.525 < z < 0.575$. The dashed line is the poor sample scaled by a constant multiple of 2.4. Cluster radius does not depend on richness.

types are remarkably similar, one being a scalar multiple of the other (Fig. 3). In other words, rich clusters do not appear to have larger radii than poor clusters, and we would obtain the same results whether we use a fixed cluster radius of 1.5Mpc or a scaling radius such as R_{30}.

To calculate a cluster's blue fraction, we use the equation:

$$f_B = \frac{n(blue,cluster+field)-n(blue,field)}{n(total,cluster+field)-n(total,field)}$$

with obvious meanings for the symbols. $n(blue, cluster + field)$ and $n(total, cluster + field)$ are determined by counting the number of blue galaxies and the total number of galaxies within $R_{1.5}$ of the cluster's BCG, and within a redshift slice of $\Delta z = 0.06$. The error in f_B is predominantly due to the statistical variation of the background. This gives us an estimation of the amount of variation that is present in the field at a particular redshift. The error in the amount of variation in the background is estimated by taking the median absolute deviation (MAD) of the measured f_B values for the 25 field samples. We chose using MAD over standard distribution because we found that the galaxies in the field don't follow a normal distribution and occasionally present radical outliers, greatly skewing the data.

3.2. *Dependence on Redshift*

To test for the Butcher-Oemler effect, we analyze how the relative blue-fraction of a cluster's galaxy population depends on redshift. Due to the large size of our sample, we bin the data by redshift and compute the weighted mean of each bin (Fig. 4). A clear linear trend is observed showing cluster blue-fraction to increase with redshift, thus confirming the presence of the Butcher-Omeler effect in our cluster sample out to $z = 0.80$. In Figure 5 we divide the sample so that there is an equal number of points in each bin, showing both clusters (open points) and field (open points). It is interesting to note that the same trend is not as provalent in the surrounding field, suggesting that passive galactic evolution due to an aging stellar population is not the primary factor in cluster evolution. It should be noticed that the best fits for the cluster and field samples intersect at $z \approx 0.85$, and could possibly indicate a period in the early universe when galaxy clusters first started to evolve.

The possibility arises that the Butcher-Oemler effect may be artificially caused from comparing dissimilar clusters over wide ranges of redshifts; or how many have put it "comparing apples to oranges". It is logical to assume that the physical properties of a poor cluster will greatly vary from those of a rich cluster. To test for this, we analyze how the blue fraction depends on redshift for the top 25% richest and poorest clusters in the sample (Fig. 6). Although there is more scatter, the Butcher-Oemler effect is still evident in both rich and poor cluster populations. The same trends can be seen when comparing low concentrated clusters with those of high concentration (Fig. 7). It is interesting to note how in Figure 7, clusters of high concentration generally have lower blue fractions than those of low concentrations at similar redshifts; hinting that concentration contributes to cluster color evolution. This trend is not observed with richness.

3.3. *Dependence on Richness*

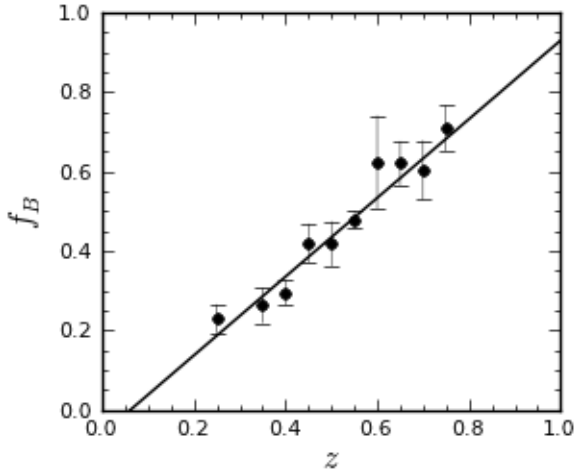

FIG. 4.—: The Butcher-Oemler effect observed in 302 galaxy clusters in the DLS. Cluster blue fraction is directly proportional to redshift. Binned by redshift in intervals of $0.05z$.

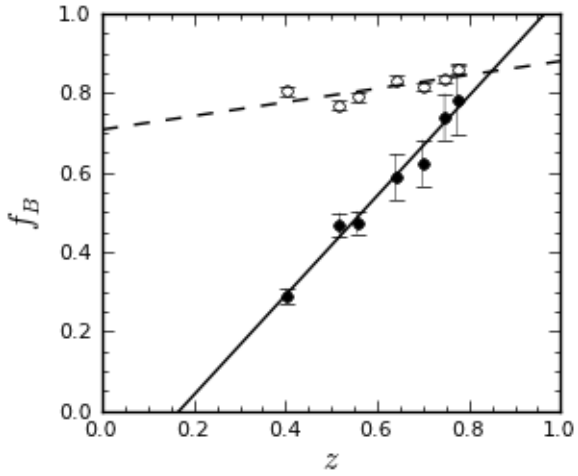

FIG. 5.—: Butcher-Oemler effect with cluster blue fraction being directly proportional to redshift. Closed points represent the complete cluster sample, open points represent the surrounding field. The data is binned by redshift with an equal number of clusters in each bin, and the weighted mean calculated for each.

When comparing blue fraction and richness in clusters of similar redshifts, we find that the blue fraction remains fairly constant (Fig. 8), suggesting richness plays a very minor role, if any, in how the colors of galaxy clusters change as a function of time. Figure 8 also shows that high redshift clusters generally have a greater blue fraction than those at low redshifts.

Figure **??** shows the gaussian of the richness distributions for clusters at low (black) and high (blue) redshifts.

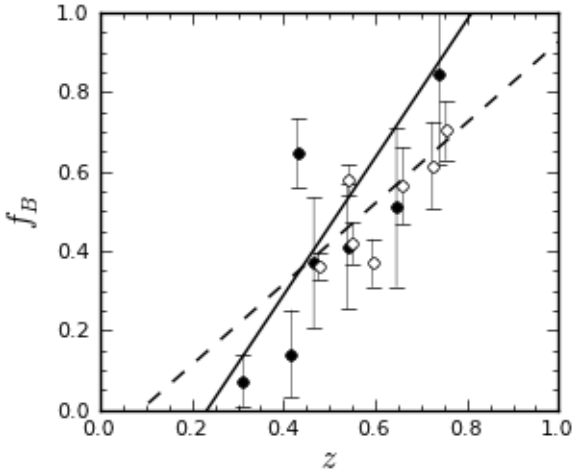

FIG. 6.—: The Butcher-Oemler effect in clusters of the poorest 25% (closed points), and the richest 25% (open points).

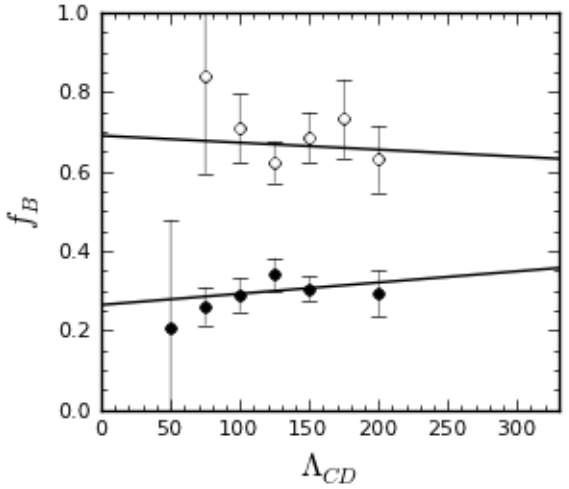

FIG. 8.—: Cluster blue fraction as a function of richness for low (closed points) and high (open points) redshifts.

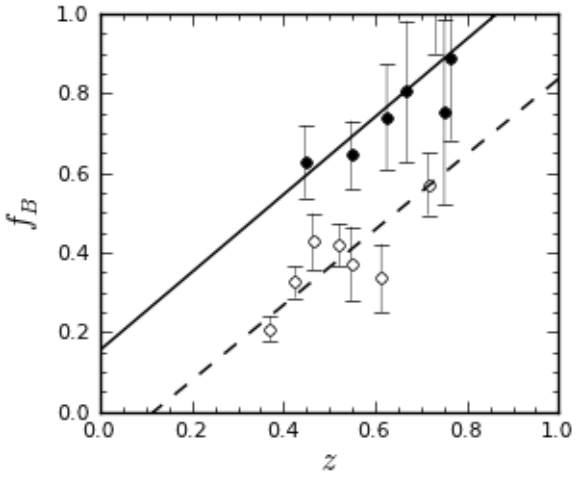

FIG. 7.—: The Butcher-Oemler effect in clusters of the lowest 25% concentration (closed points), and the highest 25% concentration (open points).

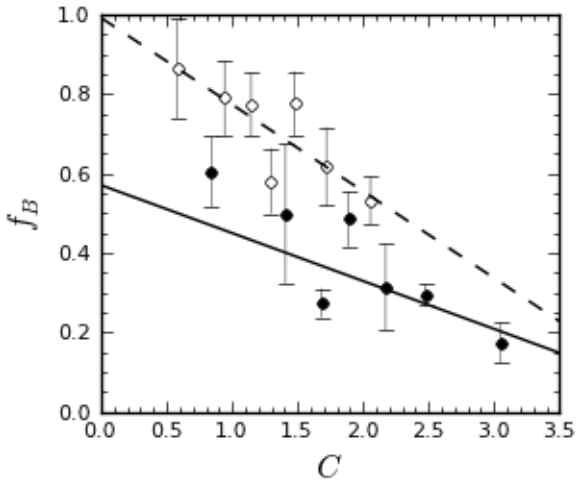

FIG. 9.—: Cluster blue fraction as a function of concentration for low ($z < 0.5$) and high ($z > 0.6$) redshifts.

We observe that at high redshift, the cluster population has relatively more high-richness clusters than those at low redshift. The observation that clusters become poorer over time suggests that galaxy-galaxy merging within cluster environments is frequent. As two galaxies merge into one, the overall richness of the cluster will decrease.

3.4. *Dependence on Concentration*

Studying how $f_B$depends on concentration may give insight as to the processes taking place within galaxy clusters, and potentially explain the amount of evolution we observe to be happening over time. A comparison between concentration and blue fraction for clusters of similar redshifts reveals a clear linear trend with f_B being inversly proportional to C (Fig. 9). It is interesting that the slope of the fit for this relation is steeper for high redshift ($z > 0.6$) clusters, than for those at lower redshifts. Clusters of low concentration show the greatest amount of color evolution with redshift, and could be due to becoming more concentrated over time. It is interesting to note that the highest concentrated clusters are only present at lower redshifts, $z < 0.5$.

4. DISCUSSION

In an attempt to determine how greatly redshift, concentration, richness, and passive evolution contribute to overall cluster evolution, we fit a theoretical model to

mathematically explain the observed data. We perform a least-squares fit to fit a general function: $Az^{\alpha} + c$ and determine $= 0.997, \alpha = 1.481, c = 0.070$ to be the best fitting model with a reduced $\chi^2 = 1.029$. We tried fitting functions using one to three parameters for z, C, Λ_{CD} and found that z was the primary factor when determining blue fraction.

REFERENCES

S. Andreon. Some Thoughts and Some New Results about the Butcher-Oemler effect. In V. Le Brun, A. Mazure, S. Arnouts, & D. Burgarella, editor, *The Fabulous Destiny of Galaxies: Bridging Past and Present*, pages 463–+, Jan. 2006.

B. Ascaso, D. Wittman, N. Benítez, and the DLS collaboration. Detecting Galaxy Clusters in the DLS and CARS: a Bayesian Cluster Finder. *ArXiv e-prints*, Nov. 2010.

N. Benítez. Bayesian Photometric Redshift Estimation. *ApJ*, 536:571–583, June 2000. doi: 10.1086/308947.

E. Bertin and S. Arnouts. SExtractor: Software for source extraction. *A&AS*, 117:393–404, June 1996.

H. Butcher and A. Oemler, Jr. The evolution of galaxies in clusters. I - ISIT photometry of C1 0024+1654 and 3C 295. *ApJ*, 219:18–30, Jan. 1978. doi: 10.1086/155751.

H. Butcher and A. Oemler, Jr. The evolution of galaxies in clusters. V - A study of populations since Z approximately equal to 0.5. *ApJ*, 285:426–438, Oct. 1984. doi: 10.1086/162519.

D. Coe, N. Bentez, S. F. Snchez, M. Jee, R. Bouwens, and H. Ford. Galaxies in the hubble ultra deep field. i. detection, multiband photometry, photometric redshifts, and morphology. *The Astronomical Journal*, 132(2):926, 2006. URL http://stacks.iop.org/1538-3881/132/i=2/a=926.

A. Dressler. The Evolution of Galaxies in Clusters. *ARA&A*, 22: 185–222, 1984. doi: 10.1146/annurev.aa.22.090184.001153.

A. Dressler and J. E. Gunn. Spectroscopy of galaxies in distant clusters. II - The population of the 3C 295 cluster. *ApJ*, 270: 7–19, July 1983. doi: 10.1086/161093.

E. Ellingson, H. Lin, H. K. C. Yee, and R. G. Carlberg. The Evolution of Population Gradients in Galaxy Clusters: The Butcher-Oemler Effect and Cluster Infall. *ApJ*, 547:609–622, Feb. 2001. doi: 10.1086/318423.

W. A. Joye and E. Mandel. New Features of SAOImage DS9. In H. E. Payne, R. I. Jedrzejewski, & R. N. Hook, editor, *Astronomical Data Analysis Software and Systems XII*, volume 295 of *Astronomical Society of the Pacific Conference Series*, pages 489–+, 2003.

R. J. Lavery and J. P. Henry. Evidence for galaxy-galaxy interactions as an active agent of the 'Butcher-Oemler' effect at a redshift of 0.2. *ApJ*, 330:596–600, July 1988. doi: 10.1086/166496.

V. E. Margoniner and D. M. Wittman. Photometric Redshifts and Signal-to-Noise Ratios. *ApJ*, 679:31–51, May 2008. doi: 10.1086/528365.

V. E. Margoniner, R. R. de Carvalho, R. R. Gal, and S. G. Djorgovski. The Butcher-Oemler Effect in 295 Clusters: Strong Redshift Evolution and Cluster Richness Dependence. *ApJ*, 548:L143–L146, Feb. 2001. doi: 10.1086/319099.

H. Mo, F. van den Bosch, and S. White. *Galaxy Formation and Evolution*. Cambridge University Press, 2010.

K. D. Rakos, T. I. Maindl, and J. M. Schombert. Photometric Signatures of Starbursts in Interacting Galaxies and the Butcher-Oemler Effect. *ApJ*, 466:122–+, July 1996. doi: 10.1086/177497.

D. J. Schlegel, D. P. Finkbeiner, and M. Davis. Maps of Dust Infrared Emission for Use in Estimation of Reddening and Cosmic Microwave Background Radiation Foregrounds. *ApJ*, 500:525–+, June 1998. doi: 10.1086/305772.

K.-V. H. Tran, P. van Dokkum, G. D. Illingworth, D. Kelson, A. Gonzalez, and M. Franx. Infall, the Butcher-Oemler Effect, and the Descendants of Blue Cluster Galaxies at z˜0.6. *ApJ*, 619:134–146, Jan. 2005. doi: 10.1086/426427.

D. M. Wittman, J. A. Tyson, I. P. Dell'Antonio, A. Becker, V. Margoniner, J. G. Cohen, D. Norman, D. Loomba, G. Squires, G. Wilson, C. W. Stubbs, J. Hennawi, D. N. Spergel, P. Boeshaar, A. Clocchiatti, M. Hamuy, G. Bernstein, A. Gonzalez, P. Guhathakurta, W. Hu, U. Seljak, and D. Zaritsky. Deep lens survey. In J. A. Tyson & S. Wolff, editor, *Society of Photo-Optical Instrumentation Engineers (SPIE) Conference Series*, volume 4836 of *Society of Photo-Optical Instrumentation Engineers (SPIE) Conference Series*, pages 73–82, Dec. 2002. doi: 10.1117/12.457348.

E. L. Wright. A Cosmology Calculator for the World Wide Web. *PASP*, 118:1711–1715, Dec. 2006. doi: 10.1086/510102.